PNAS RESEARCH ARTICLE | IMMUNOLOGY AND INFLAMMATION OPEN ACCESS

Therapeutic IgG- and IgM-specific proteases disarm the acetylcholine receptor autoantibodies that drive myasthenia gravis pathology

Alexandra C. Bayer[a,b], Liliana M. Sanmarco[c], Alex Pellerin[c], Gianvito Masi[a,b], Agustin Plasencia[c], Jordan M. Anderson[c], Richard J. Nowak[a], Valentina Damato[d], Luca Massacesi[d], Minh C. Pham[b], Fatemeh Khani-Habibabadi[a,b], Heather Vital[c], Nathan Higginson-Scott[c], Kevin L. Otipoby[c], Yi Xing[c], Ivan D. Mascanfroni[c,1], and Kevin C. O'Connor[a,b,1]

Affiliations are included on p. 11.

Edited by Lawrence Steinman, Stanford University Beckman Center for Molecular and Genetic Medicine, Stanford, CA; received March 17, 2025; accepted September 4, 2025

Myasthenia gravis (MG) is an autoimmune disorder caused mainly by autoantibodies against the acetylcholine receptor (AChR), leading to muscle weakness. While treatments targeting AChR autoantibodies benefit many, some patients remain refractory, highlighting the need for personalized therapies. This study evaluates the therapeutic potential of S-1117, a pan-IgG-specific protease, in AChR autoantibody-mediated pathology. Using live cell-based assays, we examined AChR-specific monoclonal IgG autoantibodies (mAbs) and patient-derived serum samples for their effects on receptor binding, blockade, internalization, and complement activation, before and after treatment with S-1117. S-1117 effectively removed the crystallizable fragment (Fc)γ from both mAbs and serum IgG, impairing Fcγ-mediated complement activation in both soluble and antigen-bound forms. In cases with partial complement reduction, AChR-specific IgM contributed to complement deposition. AChR-IgM acted in concert with IgG in some patients to enhance complement deposition, while acting as main complement driver in others. An IgM-specific protease completely suppressed the pathogenic effects of AChR-IgM in two independent patient cohorts. These findings highlight the therapeutic potential of S-1117 in neutralizing AChR-IgG Fcγ-mediated effector functions and reveal an MG subset driven by IgM pathology. Our study shows that targeting both IgG- and IgM-mediated mechanisms with therapeutic proteases provides an approach to MG treatment and establishes a framework for patient stratification based on disease mechanisms, advancing precision medicine in MG.

autoimmune disease | myasthenia gravis | immunoglobulins (Ig)-proteases | pathogenic IgM | complement

Acetylcholine receptor (AChR)-specific autoantibodies, prevalent in a large subset of myasthenia gravis (MG) patients, have been established to disrupt neuromuscular signal transmission through three primary pathogenic mechanisms (1–9): i) antibody-dependent complement deposition, ii) AChR crosslinking, leading to receptor internalization and degradation (antigenic modulation), and iii) acetylcholine binding site blockade (receptor antagonism). Predominantly, AChR autoantibodies are of the immunoglobulin (Ig) G isotype (AChR-IgG) (2, 10, 11), comprising various IgG subclasses (12–17). Nevertheless, AChR-IgM and IgA are also detected in MG patients, albeit at lower titers compared to IgG (18–20). Our previous findings have shown that approximately 80% of MG patients exhibit detectable in vitro AChR autoantibody-mediated complement deposition (20) which, combined with reports indicating a 60 to 70% response rate to complement inhibitors (21, 22), underscores the predominance and relevance of this mechanism in MG pathology. Current therapeutic strategies targeting AChR autoantibodies or their crystallizable fragment (Fc)-mediated effector functions include complement pathway inhibitors that disrupt membrane attack complex formation (21–23) and neonatal Fc receptor (FcRn) inhibitors that reduce circulating IgG, including antigen-specific autoantibodies, by blocking FcRn-mediated recycling (24, 25). Despite important clinical improvements achieved with these therapies, 40 to 70% (21, 25–28) of MG patients are classified as nonresponders. Intravenous Ig and plasma exchange can also target AChR autoantibodies and are usually employed during exacerbations of MG (29). However, their utility for long-term maintenance therapy is limited by the temporary nature of their therapeutic benefits and the potential for accompanying side effects (30, 31). Collectively, these findings underscore the necessity of investigating innovative therapeutic strategies that may deliver superior efficacy compared to existing options.

Significance

This study presents S-1117, an IgG-specific protease, as a promising therapeutic approach for the treatment of acetylcholine receptor-positive myasthenia gravis (AChR-MG). S-1117 was shown to efficiently cleave the Fcγ region of pathogenic AChR-IgG, thereby abrogating effector functions, most notably complement activation. Importantly, its application to serum derived from MG patients uncovered a previously unrecognized disease subset driven by pathogenic AChR-IgM, expanding our understanding of MG pathophysiology. The use of an IgM-specific protease, either alone or in combination with S-1117, effectively suppressed complement deposition in this subgroup, underscoring the need for tailored therapeutic interventions. These findings reveal critical immunopathogenic heterogeneity in MG, demonstrating the potential of Ig-specific enzymes to advance precision medicine in antibody-mediated disorders.

This article is a PNAS Direct Submission.

[1]To whom correspondence may be addressed. Email: idmascan@gmail.com or kevin.oconnor@yale.edu.

This article contains supporting information online at https://www.pnas.org/lookup/suppl/doi:10.1073/pnas.2505984122/-/DCSupplemental.

Published October 21, 2025.

Within the realm of novel biologics for autoimmune diseases, Ig-degraders have emerged as a pioneering category (32, 33). These include antibody-sculpting enzymes like IdeS (IgG-degrading enzyme of *Streptococcus pyogenes*), a virulence factor in the bacterium that facilitates host immune defense evasion by diminishing phagocytosis and complement activation, promoting bacterial survival (34). IdeS acts by catalyzing the cleavage of the IgG heavy chain on the C-terminal side of the hinge region, yielding one antigen-binding $F(ab')_2$ fragment and one noncovalently linked homodimeric Fcγ fragment (35). Proteolytic removal of the Fc domain of antibodies abrogates Fcγ-dependent effector functions such as complement-dependent cytotoxicity, antibody-dependent cell-mediated cytotoxicity (ADCC), and cellular phagocytosis. Their selectivity, based on specific protein–protein interactions with the Fcγ portion of antibodies, enables remarkable specificity for IgG isotype cleavage (35–38). IdeS-based therapies, originally studied for preventing humoral renal transplant rejection in highly human leukocyte antigen-sensitized recipients (39–43), have shown promising preclinical results in autoimmune contexts. Conditionally approved in Europe, Idefirix® is used for desensitization treatment of adult kidney transplant patients and is undergoing phase 2 trials for both Guillain–Barré syndrome and Goodpasture syndrome (44–48). However, prior exposure to *S. pyogenes* in the general population may elicit a humoral memory response against IdeS (49), resulting in elevated anti-IdeS IgG levels and potential neutralization, thereby limiting its therapeutic efficacy, and precluding retreatment or long-term use (36).

In this study, we evaluate a pan-IgG-cleaving enzyme, which has been deimmunized and engineered for improved half-life by fusing it to an effector function-agnostic, auto-cleavage-resistant human IgG1 Fcγ domain. We demonstrate efficient Fcγ-cleavage of polyclonal AChR-IgG in serum from MG patients and human recombinant AChR-IgG monoclonals (mAbs) in vitro, significantly reducing complement deposition in both systems. Notably, serum treatment with the IgG-specific protease uncovered a subset of MG patients in whom complement deposition was mediated by the IgM isotype. The pathogenic role of these IgM autoantibodies was confirmed by using an IgM-specific protease, and its use, either alone or in combination with the IgG-specific protease revealed varying contributions from AChR autoantibody isotypes to MG pathogenesis. Altogether, this study provides three major insights. First, S-1117 shows therapeutic potential as an IgG-specific protease, effectively cleaving IgG—including pathogenic AChR autoantibodies—and inhibiting complement deposition that leads to tissue damage. Second, the results reveal diversity in the molecular mechanisms driving AChR-mediated pathogenic effector functions, identifying an MG disease subset characterized by pathogenic IgM. Third, the findings highlight the need for personalized treatment in AChR-MG and the promise of Ig-specific sculpting enzyme combination therapy in neutralizing diverse isotype-driven pathogenicity in this and other autoantibody-mediated diseases.

Results

S-1117 Efficiently Removes the Fcγ of Monoclonal and Serum Polyclonal AChR-Specific IgG. Five human recombinant AChR-IgG mAbs previously generated and extensively characterized by our laboratory (8) were selected from a larger repository based on their molecular and functional properties to represent diverse autoantibody profiles. These mAbs were treated with varying concentrations of S-1117 (6 μM to 0.05 μM) or left untreated for comparison. The efficacy of Fcγ cleavage was assessed using enzyme-linked immunosorbent assay (ELISA), by detecting the Fcγ present on intact IgG and single-cleaved IgG (scIgG), both of which are products present in undigested or partially digested reactions. Results show concentration-dependent cleavage of the Fcγ fragment from mAbs (Fig. 1*A*), with complete cleavage achieved at 6 μM of S-1117. Sodium dodecyl sulfate-polyacrylamide gel electrophoresis (SDS-PAGE) analysis corroborated the ELISA findings, demonstrating that at the highest concentration of S-1117 tested (6 μM), only $F(ab')_2$ and Fcγ fragments were present, with no detectable intact IgG or scIgG species (*SI Appendix*, Fig. S1*A*). Importantly, the cleavage activity of S-1117 was confirmed to be substrate-specific, as only human IgG molecules were targeted, with no detectable activity against other Ig isotypes as demonstrated by capillary electrophoresis with SDS analysis (*SI Appendix*, Fig. S1*B*). This optimal enzyme concentration (6 μM) was subsequently employed for the treatment of serum samples. To encompass the diversity of pathogenic functions, serum samples from five healthy donors and 11 AChR-MG patients were selected from a larger, previously characterized cohort (20), ensuring representation of the full range of AChR-specific IgG-mediated responses. To confirm that cleavage was due to the catalytic activity of the protease and that engineered modifications did not influence its function, an inactive form of S-1117 was included as a control in all assays. Serum samples were exposed to 6 μM of S-1117 and Fcγ cleavage was assessed by ELISA and compared to both untreated samples and samples treated with 6 μM of the inactive IgG protease. Complete cleavage of total IgG was observed in both the AChR-MG patient and healthy control serum samples ($P \leqq 0.0001$, Fig. 1*B*) following incubation with the S-1117, when compared to untreated condition or the inactive form of the protease.

To evaluate cleavage of AChR-specific IgG and its effect on autoantibody binding, live cell-based assays (CBA) were used. HEK cells expressing rapsyn-clustered human AChR were incubated with mAbs that were previously treated with either 6 μM, 1.5 μM, or 0.1 μM of S-1117, or serum samples treated with 6 μM of S-1117. Binding in tested conditions was compared to untreated controls or samples treated with the inactive form of S-1117. Concentrations selected for the mAbs treatment were chosen based on the ELISA results that showed maximal, intermediate, and minimal effects in Fcγ cleavage, respectively. Detection of Fcγ cleavage, after treatment with S-1117, was assessed using an anti-Fcγ secondary antibody in the CBA. Consistent with the ELISA results, flow cytometry CBA revealed a concentration-dependent reduction in Fcγ detection across all recombinant mAbs (Fig. 1*C*). Complete cleavage was achieved at 6 μM of S-1117, resulting in the exclusive detection of AChR-$F(ab')_2$ fragments binding to transfected cells, as observed by microscopy (Fig. 1*D*).

In serum samples from AChR-MG patients treated with S-1117, a significant reduction in AChR-IgG binding was confirmed compared to untreated samples ($P = 0.0085$) or those treated with the inactive protease ($P = 0.0056$) (Fig. 1*E*). As anticipated, no AChR-IgG binding was detected in healthy donor samples under any tested condition. Fcγ detection in samples treated with the inactive protease remained comparable to the levels obtained in untreated samples, confirming the specificity of S-1117.

We next assessed the binding capacity of generated AChR-specific $F(ab')_2$ fragments from mAbs and serum samples using CBA, followed by $F(ab')_2$ detection through microscopy and flow cytometry. Microscopy confirmed the presence of AChR-$F(ab')_2$ fragments bound to transfected cells (Fig. 1*D*), and flow cytometry provided quantitative evidence of comparable $F(ab')_2$ binding across all tested conditions for both mAbs (Fig. 1*F*) and AChR-MG serum samples (Fig. 1*G*). No $F(ab')_2$ binding to

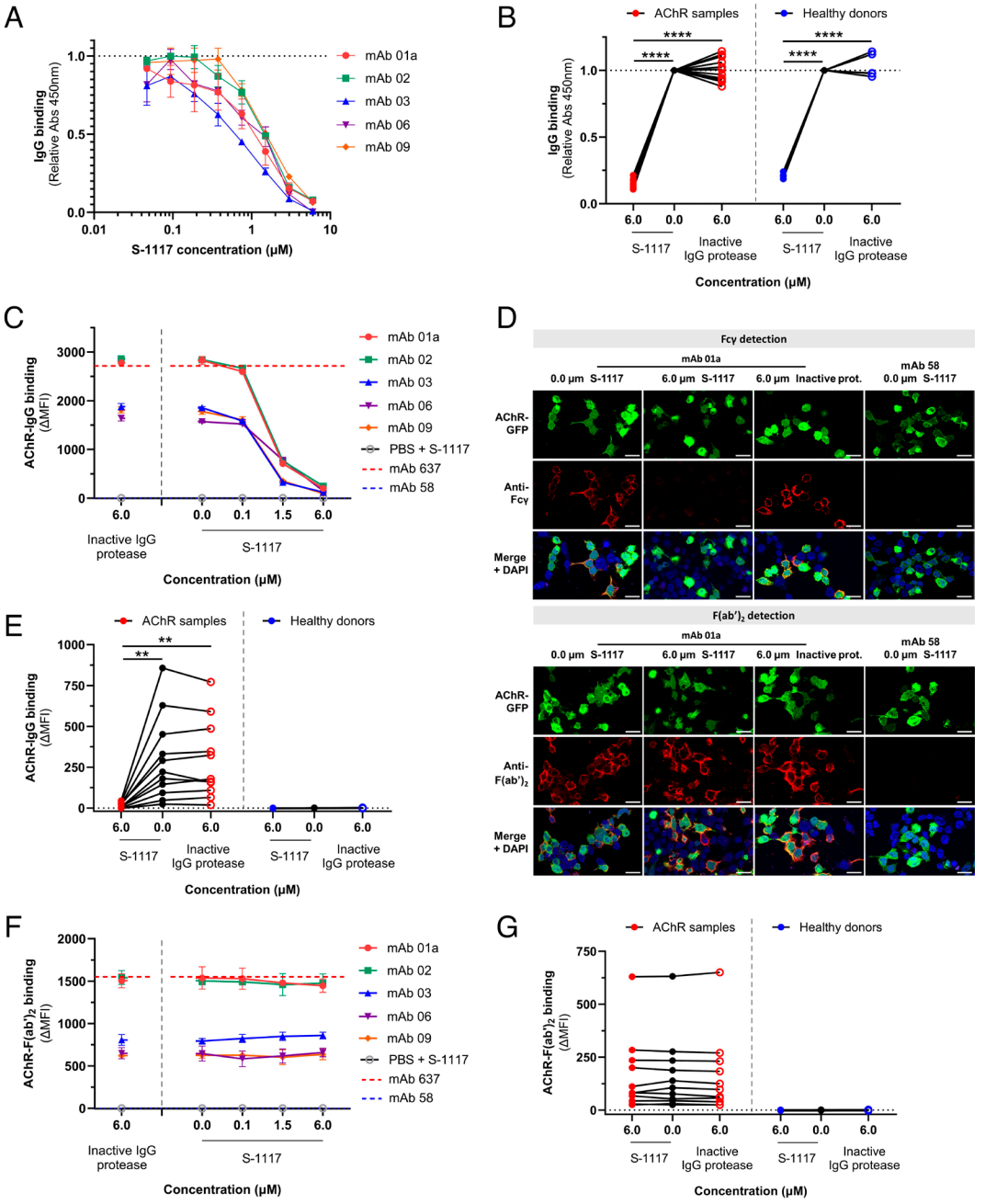

Fig. 1. Efficacy of S-1117-mediated IgG Fcγ cleavage and its effect on AChR autoantibody binding capacity. AChR-IgG mAbs or serum samples were treated with the S-1117 protease to generate separate Fcγ and F(ab′)$_2$ fragments. Five AChR-IgG mAbs were incubated with varying concentrations of S-1117 (active protease), or with an inactive form of S-1117 or left untreated. Serum samples of 11 AChR-MG or five healthy donors were treated with maximum concentration of S-1117, or an inactive form of S-1117 or left untreated. (*A* and *B*) Plots showing IgG binding for (*A*) mAbs and (*B*) serum samples, after S-1117 treatment. Binding was evaluated by ELISA through the detection of Fcγ fragments from residual intact IgG or scIgG. ELISA results are presented as relative absorbance, with untreated samples normalized to 1 (horizontal black dotted line). (*C*) Plot depicting AChR-IgG binding for mAb samples following S-1117 treatment. Binding was evaluated using a clustered cell-based assay (CBA) by measuring Fcγ fragments of intact or scIgG remaining after cleavage, by flow cytometry. (*D*) Indirect immunofluorescence staining detecting AChR-IgG binding of a representative AChR-mAb (mAb 01a) following S-1117 treatment and a negative control (mAb 58). First row and fourth rows: HEK293T expressing AChR-GFP. Second and fifth rows: IgG binding (red) detected through Fcγ or F(ab′)$_2$ specific staining, respectively. Third and sixth rows: merge with DAPI, confirming colocalization of AChR-IgG (when detected) with AChR-expressing cells. All images were captured at 63× magnification (Scale bar: 20 μm). (*E*) Plot depicting AChR-IgG binding for serum samples following S-1117 treatment; the assay was performed as described in (*C*). (*F* and *G*) Plots illustrating the binding capacity of F(ab′)$_2$ fragments from (*F*) mAbs and (*G*) serum samples, following S-1117 treatment. Binding was assessed using a CBA with detection performed using a secondary antibody specific for the F(ab′)$_2$ fragments, by flow cytometry. Flow cytometry CBA results are shown as ΔMFI (corrected mean fluorescence intensity). The negative control mAb 58 (AQP4-specific, horizontal blue dotted line) and positive control mAb 637 (AChR-specific, horizontal red dotted line) were included in all mAb CBAs. For the serum CBAs, mean values from healthy donors are represented by a horizontal black dotted line. Each data point represents the mean of triplicate measurements, with error bars indicating the SEM. Statistical differences are shown when significant.

AChR was detected in the healthy donor samples, confirming absence of AChR-IgG in these samples.

Altogether, these findings provide robust evidence that the engineered protease S-1117 efficiently cleaves the Fcγ fragment from both total IgG and AChR-IgG. The cleavage efficacy is concentration-dependent, occurs with high specificity, without influence from the engineered modifications, and does not impair autoantibody binding to AChR.

Treatment with S-1117 Has Limited Impact on Fcγ-Independent Pathogenic Mechanisms of AChR-IgG. AChR-IgG-mediated pathogenicity can be divided into Fcγ-dependent mechanisms, such as complement activation, and Fcγ-independent mechanisms, like receptor blockade and internalization, which rely solely on the Fab portion of the molecule. Following confirmation of effective cleavage by the protease, we assessed the ability of the resulting cleaved products to exert Fcγ-independent pathogenic mechanisms (Fig. 2*A*).

First, we evaluated whether treatment with S-1117 could affect the intrinsic blocking activity of the studied AChR mAbs or serum samples derived from patients. AChR autoantibodies are categorized as blockers when they interfere with acetylcholine binding to its cognate site on the receptor. To quantify this, we utilized a clustered live AChR CBA and fluorescence-conjugated α-bungarotoxin (αBTX), a neurotoxic peptide that binds with high affinity to the acetylcholine binding site on AChR (7, 50). While αBTX binding is a well-established surrogate for assessing antibody-mediated blockade at this site, it is important to note that it provides only an indirect approximation of acetylcholine antagonism, as it does not account for differences in ligand size, binding kinetics, or alternative inhibitory mechanisms (51). Consistent with previous findings (8), two out of the five tested mAbs (mAb 01a and 03) demonstrated robust blocking capacity, markedly reducing αBTX signal compared to the negative controls (no antibody; non-AChR-specific autoantibody, mAb 58; or nonblocking AChR autoantibody, mAb 637). The blocking efficiency was comparable between protease-treated and untreated conditions (Fig. 2*B*). Human sera from healthy donors

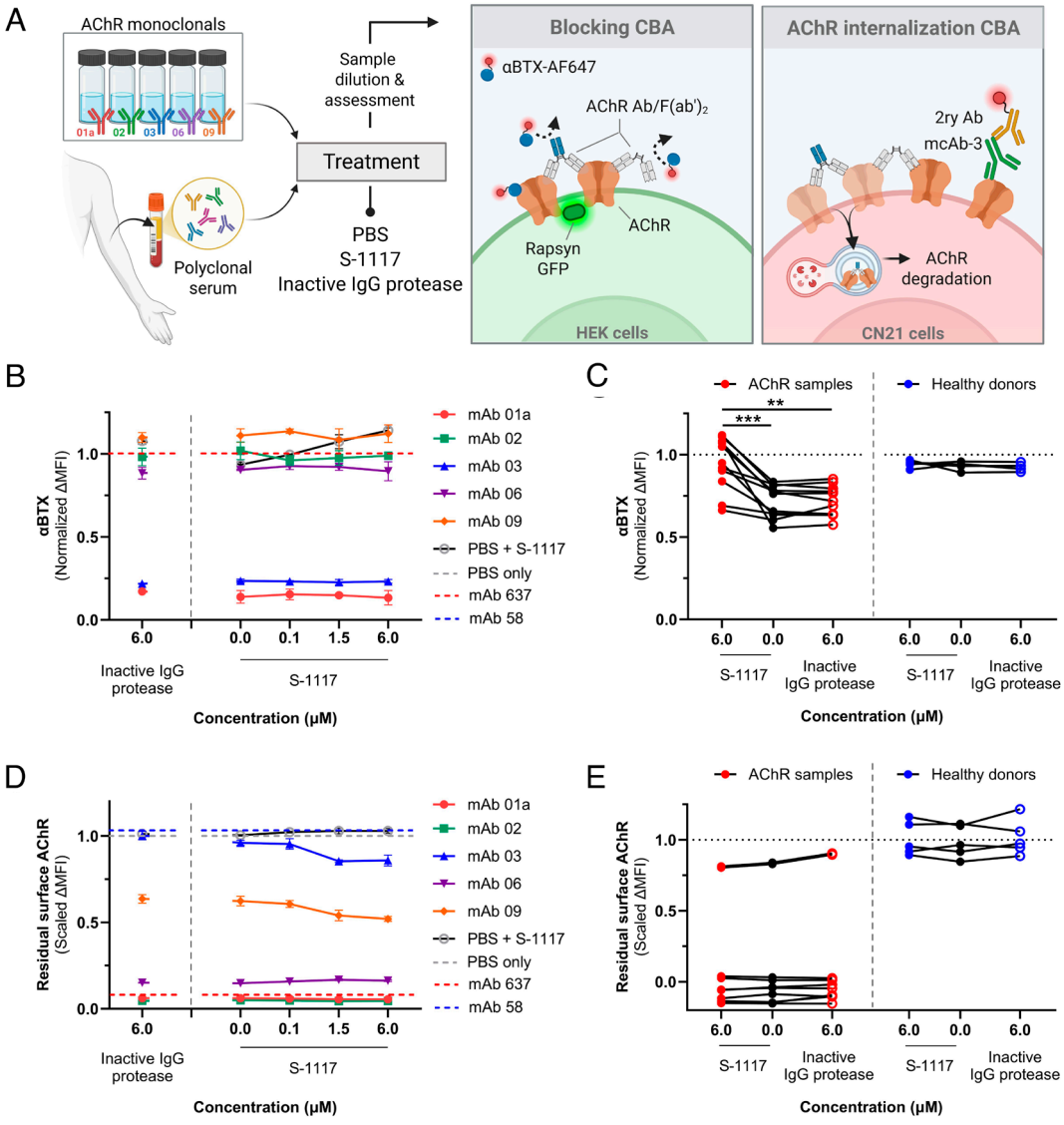

Fig. 2. Effect of S-1117 on AChR autoantibody Fcγ-independent pathogenic mechanisms. The ability of AChR autoantibodies to block the acetylcholine binding site or mediate receptor internalization was assessed with five AChR-IgG mAbs, 11 AChR-MG serum, and five healthy donor serum samples after incubation with S-1117 (active protease), an inactive form of S-1117, or no treatment using tailored CBA and flow cytometry assessment. (*A*) Experimental outline: Schematic of sample treatment followed by blocking and AChR internalization assessment. (*B* and *C*) Plots showing αBTX binding to AChR following incubation with (*B*) mAbs and (*C*) serum samples, as a measure of blocking capacity. The αBTX signal was expressed as ΔMFI (corrected mean fluorescence intensity) and normalized to the negative control (no mAb added, ΔMFI = 1, horizontal black dotted line). (*D* and *E*) Plots showing residual surface AChR following incubation with (*D*) mAbs and (*E*) serum samples, as a measure of internalization capacity. Residual surface AChR was detected using the anti-human AChR mcAb-3 antibody, with the signal expressed as ΔMFI (corrected mean fluorescence intensity) and scaled to the negative control (no mAb added, ΔMFI = 1, horizontal black dotted line). For both assays, unstained controls were set to the lower limit (ΔMFI = 0). Controls mAb 58 (AQP4-specific, blue dotted line) and mAb 637 (AChR-specific, red dotted line) were included in all mAb CBAs. Each data point represents the mean of triplicate measurements, with error bars showing SEM. Statistical differences are shown when significant. AChR: Acetylcholine receptor, Ab: antibody, $F(ab')_2$: antigen-binding fragment, 2ry: secondary, αBTX: alpha-bungarotoxin, GFP: Green fluorescent protein, AF647: Alexa Fluor 647, PBS: Phosphate-buffered saline, HEK: Human embryonic kidney.

exhibited no detectable blocking activity, whereas sera from AChR-MG patients showed variable degrees of blocking activity, as expected (20). Incubation of AChR serum samples with S-1117 reduced the observed blocking capacity compared to untreated samples (P = 0.0009) or samples treated with the inactive protease (P = 0.0014) (Fig. 2*C*).

To assess the impact of protease treatment on the capacity of the mAbs or serum samples to induce AChR internalization (also referred to as antigenic modulation), we employed a tailored CBA that detects residual AChR on the cell surface following incubation with the samples, using the mouse anti-human AChR mcAb-3 (52). This approach avoids the use of αBTX and, so, the simultaneous detection of receptor blockade and internalization, allowing for a much clearer signal coming only from the latter pathogenic mechanism. Consistent with previous characterization of the tested mAbs (8), four out of five mAbs (all except mAb 03) exhibited internalization capacity, which was unaffected by protease treatment (Fig. 2*D*). Serum from healthy donors displayed no measurable internalization capacity, whereas serum from MG patients showed variable internalization capacity levels. The internalization capacities of AChR autoantibodies in these serum samples were not altered by protease treatment (Fig. 2*E*). Collectively, these findings show that treatment with S-1117 preserves antibody Fcγ-independent properties, including binding, blocking, and receptor internalization, for both mAbs and serum samples.

Treatment with S-1117 Effectively Reduces AChR-IgG-Mediated Complement Deposition. To evaluate the impact of S-1117 on the classical complement pathway activation, we employed the clustered live AChR CBA, tailored to detect C3b, which is a key subproduct of complement cascade activation that binds to cell membranes, allowing identification of cells on which deposition has occurred (Fig. 3*A*). Consistent with our previous characterizations (8), four out of five mAbs mediated complement deposition, two at high levels (mAb 01a and 02) and two at moderate levels (mAb 03 and 09). Low C3b deposition was detected for mAb 06 (*SI Appendix*, Fig. S2*A*). Incubation with S-1117 led to varying degrees of reduction in C3b deposition, with significant reduction only observed in samples treated with 0.1 μM S-1117 (P = 0.0336 compared to untreated samples and P = 0.0452 compared to samples treated with the inactive protease, Fig. 3*B*). Unexpectedly, C3b deposition was more effectively diminished at the lower S-1117 concentration (0.1 μM) compared to higher concentrations (1.5 μM and 6 μM), despite the latter mix containing lower levels of intact IgG (Fig. 1*C*) and consequently higher amounts of cleaved $F(ab')_2$.

These findings led us to hypothesize that the $F(ab')_2$ fragments, generated through digestion, might recruit other molecules, such as anti-$F(ab')_2$ antibodies from the normal human serum (NHS), which serves as a standardized complement source in the assay, thereby triggering complement activation and C3b deposition. To test this, we repeated the C3b CBA experiment using a mAb treated with different concentrations of S-1117 and either undigested or S-1117-digested NHS as the complement source. Undigested NHS reproduced the pattern previously observed, with higher C3b levels for mAbs samples treated with higher concentrations of S-1117. In contrast, using digested NHS in the assay abrogated this effect, enabling a more accurate assessment of the impact of Fcγ removal in the complement deposition assay (*SI Appendix*, Fig. S2*B*). Under this condition, even the lowest concentration of S-1117 tested (0.1 μM) markedly reduced complement deposition, with increasing concentrations of S-1117 resulting in further (near-complete) reduction of complement deposition. These results confirm that components within the IgG fraction of NHS can enhance complement activation by supplying $F(ab')_2$ fragments with a surrogate Fcγ region. To further define these interactions and to confirm they were mediated by anti-$F(ab')_2$ antibodies, we generated $F(ab')_2$ fragments by enzymatic digestion of mAbs with S-1117 and removed residual Fcγ fragments using Protein G beads. The purified $F(ab')_2$ fragments were then used as targets to assess the reactivity of the isolated IgG fraction from NHS, using both ELISA and CBA. To control for nonspecific binding due to the high IgG concentrations tested, an isotype-matched control antibody with irrelevant specificity was included at equivalent concentrations. In both assays, NHS-derived IgG bound specifically and in a concentration-dependent manner to the $F(ab')_2$ fragments, confirming the presence of anti-$F(ab')_2$ antibodies in NHS (*SI Appendix*, Fig. S3 *A* and *B*).

In the assays using human sera, assessment of C3b deposition using healthy donor serum samples showed no detectable C3b levels, and protease treatment did not alter these baseline levels. Serum samples from AChR-MG patients exhibited heterogeneous complement deposition capacities, with significant reductions in C3b levels observed after incubation with S-1117 compared to untreated samples (P = 0.0028) or samples treated with the inactive protease (P = 0.0024) (Fig. 3*C*). This effect was confirmed to be associated with Fcγ fragment removal, as treatment with the inactive IgG protease control, did not impact complement deposition when compared to untreated condition.

Furthermore, to investigate the pathophysiological environment in which S-1117 would function, we evaluated its ability to cleave and inhibit C3b deposition after AChR autoantibodies had already bound to their antigen and performed in situ digestion. To that end, we preincubated AChR-expressing HEK cells with serum samples from healthy donors or AChR-MG patients, allowing AChR autoantibodies to bind the target before introducing the protease (Fig. 3*A*). Incubation of S-1117 with preformed immune complexes resulted in a significant reduction in complement deposition in patient samples ($P \leqq 0.0001$ vs. untreated and inactive protease, Fig. 3*D*). Altogether, these findings underscore the ability of S-1117 to disrupt complement activation by efficiently cleaving Fcγ fragments from both soluble and antigen-bound autoantibodies.

AChR-IgM Triggers Complement Deposition in a Subset of AChR-MG Patients and Is Efficiently Neutralized by an IgM-Specific Protease. Following treatment with S-1117, most serum samples exhibited a significant reduction in AChR-mediated complement deposition. However, one patient (MG-01) showed considerable residual C3b deposition despite effective IgG cleavage (Fig. 4*A*). In the classical complement pathway, activation can be initiated by immune complexes formed by IgG and IgM antibodies recognizing their target antigen (53–55). We hypothesized that this patient might have antigen-specific IgM contributing to complement activation and screened the sample for AChR autoantibodies of various isotypes (IgG, IgM, IgA) using isotype-specific CBA (20). MG-01 presented detectable AChR-IgG and IgM binding, as shown by microscopy CBA (Fig. 4*B*) and confirmed by flow cytometry (Fig. 4*C*). The latter further demonstrated that AChR-IgM levels in MG-01 were the highest among the tested AChR-MG cohort.

To elucidate the role of AChR-IgM in complement activation for this patient, we incorporated an IgM-specific protease into our experimental design. This protease selectively degrades IgM antibodies in a dose-dependent manner without affecting other Ig isotypes (*SI Appendix*, Fig. S4 *A* and *B*). Serum samples were incubated with S-1117, the IgM-specific protease, or both enzymes combined, and C3b deposition was compared to the untreated

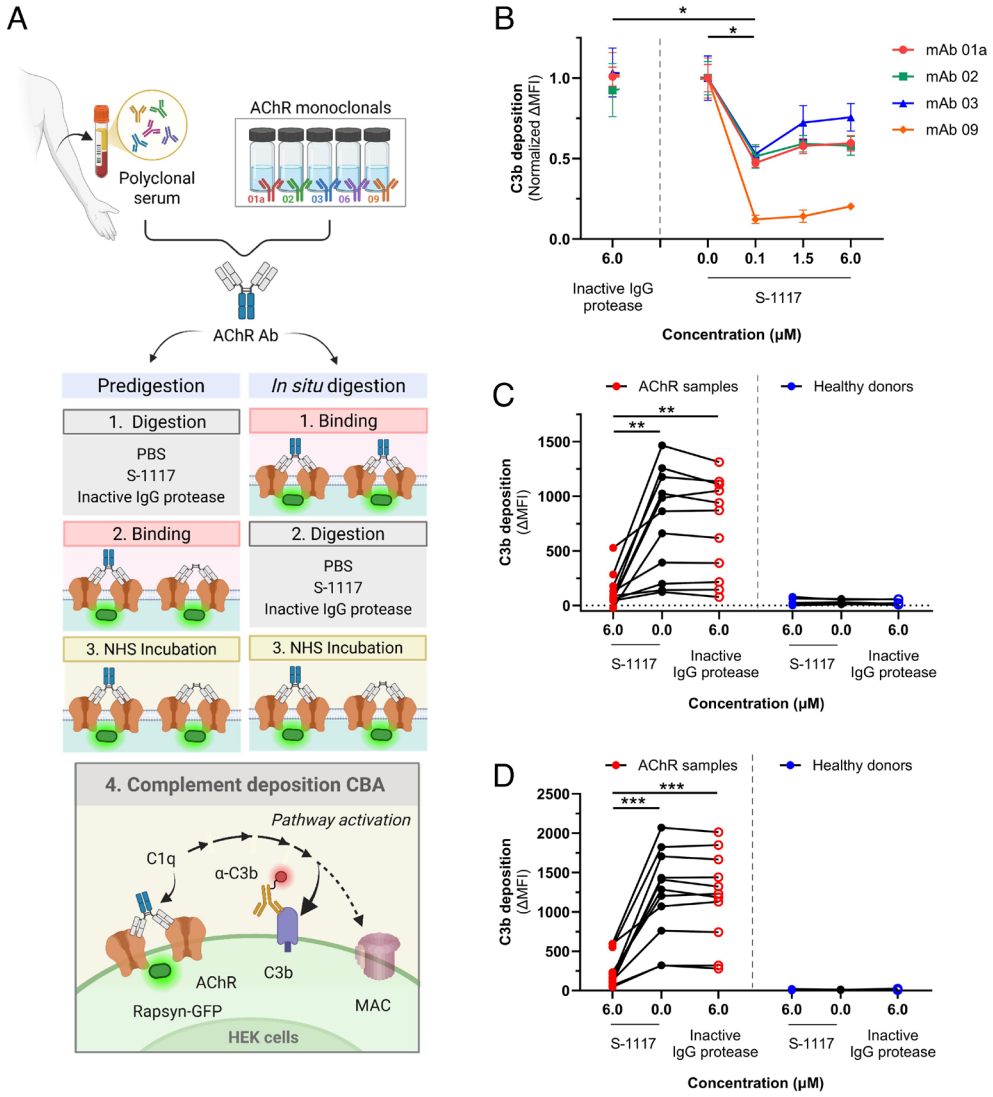

Fig. 3. Effect of S-1117 on both soluble and antigen-bound AChR autoantibody-mediated complement deposition. The capacity of AChR autoantibodies to induce complement deposition was assessed using five AChR-IgG mAbs, serum samples from 11 AChR-MG patients and five healthy donors. Samples were incubated with S-1117 (active protease), an inactive form of S-1117, or left untreated, and the effects were analyzed using tailored CBA. (*A*) Experimental outline: Schematic of sample treatment followed complement deposition assessment. (*B* and *C*) Plots depicting complement deposition capacity for (*B*) mAbs and (*C*) serum samples, detected using an anti-human C3b secondary antibody following protease treatment. (*D*) Complement deposition levels determined after in situ cleavage of prebound AChR autoantibodies from serum samples. C3b deposition levels for mAbs are shown as normalized ΔMFI (corrected median fluorescence intensity) relative to untreated samples (ΔMFI = 1), while for serum samples, they are expressed as non-normalized ΔMFI values. The mean value for healthy donor sera is indicated by a horizontal black dotted line. Each data point represents the mean of triplicate measurements, with error bars representing the SEM. Statistical differences are shown when significant. AChR: Acetylcholine receptor, GFP: Green fluorescent protein, C3b: Complement component 3b, α-C3b: anti-C3b antibody, C1q: Complement component 1q, MAC: Membrane attack complex, NHS: Normal human serum, PBS: Phosphate-buffered saline, HEK: Human embryonic kidney.

condition or those treated with the inactive form of S-1117. A schematic representation illustrating the selective cleavage of AChR-IgG and AChR-IgM by their respective proteases is shown in Fig. 4*D*. This diagram highlights which antibody isotypes remain active, and which are functionally disarmed under each treatment condition. Consistent with prior observations, IgG degradation alone resulted in a partial reduction of complement deposition (approximately 40%, $P = 0.0027$ vs. untreated; $P = 0.0028$ vs. inactive protease). In contrast, IgM degradation alone led to a more substantial reduction (approximately 60%, $P \leqq 0.0001$ vs. untreated and inactive protease). Simultaneous treatment with both proteases completely abolished complement deposition in the sample ($P \leqq 0.0001$ vs. untreated and inactive protease, Fig. 4*E*).

We initially detected AChR-IgM in patient MG-01 during analysis of a cohort of 11 AChR-MG patients. To assess the broader prevalence of AChR-IgM, we subsequently screened 210 additional AChR-MG patients, analyzing a total of 330 serum samples (including longitudinal collections). In this expanded cohort, we identified 26 AChR-IgM-positive samples from 20 patients. Together with MG-01, this yielded 27 positive samples from 21 patients (MG-01 to MG-21), corresponding to a frequency of 9.5% (21/221) of AChR-MG patients harboring detectable AChR-IgM autoantibodies (*SI Appendix*, Fig. S5*A*).

Using the experimental conditions described above for MG-01, we treated AChR-IgM-positive serum samples with S-1117, the IgM-specific protease or both proteases, and assessed C3b deposition to evaluate the functional relevance of AChR-IgM in complement activation. Among the 27 samples analyzed, four samples (all from patient MG-21) demonstrated no detectable complement activation (*SI Appendix*, Fig. S6*A*). This outcome was anticipated, as all four samples demonstrated low AChR-specific IgG binding in the CBA.

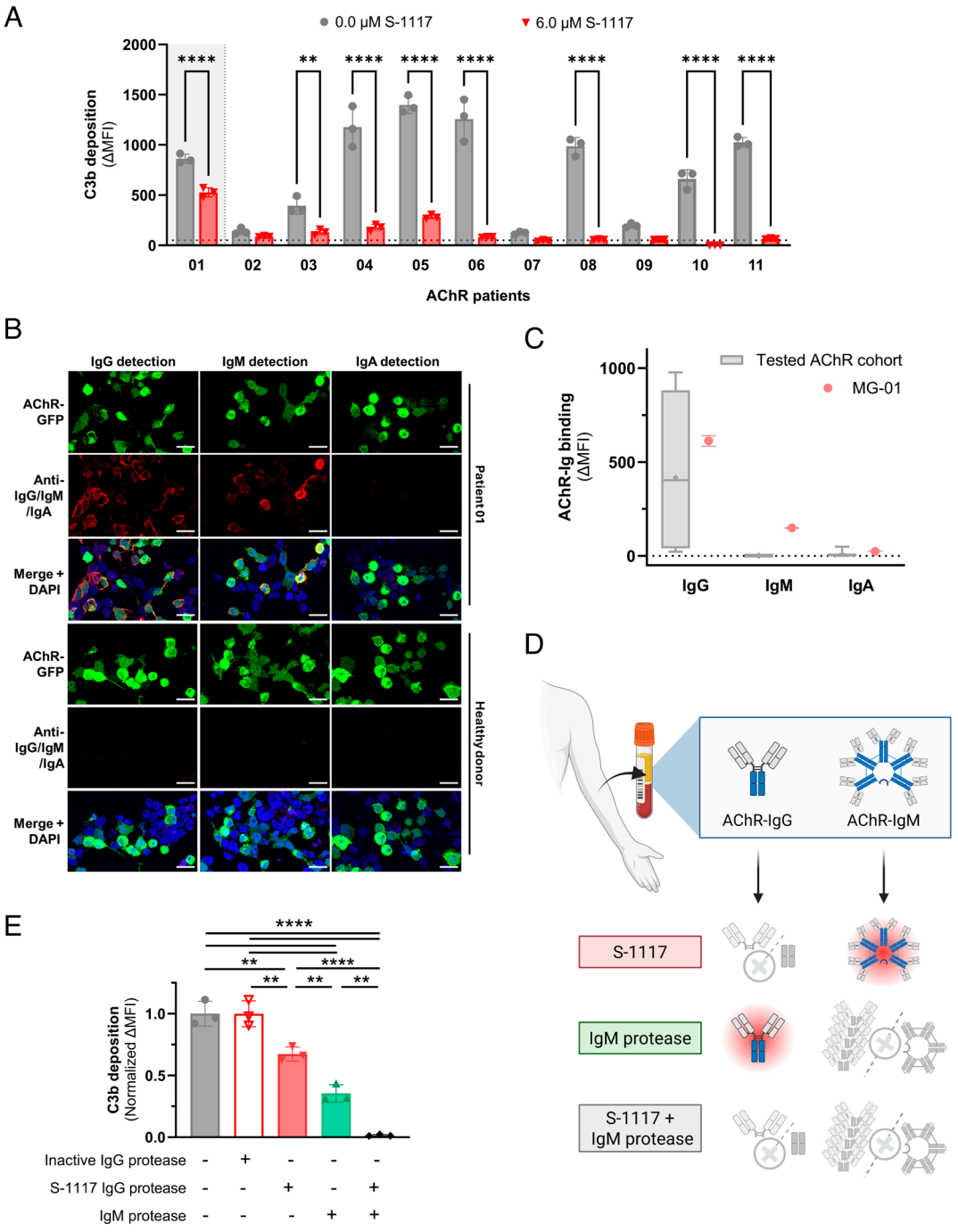

Fig. 4. Contribution of serum AChR-IgM autoantibodies to complement deposition. (*A*) Bar graph showing complement deposition levels (ΔMFI = corrected median fluorescence intensity) in 11 AChR MG serum samples, incubated with or without S-1117. CBA tailored to measure C3b deposition with an anti-human C3b secondary antibody was employed. The mean value of healthy donor serum (n = 5) is indicated by a horizontal black dotted line, and the gray section highlights the profile of patient MG-01, demonstrating partial reduction of C3b deposition following protease treatment. (*B*) Indirect immunofluorescence staining detecting AChR-IgG, IgM, and IgA in serum samples of patient MG-01 and a representative healthy donor. First row and fourth rows: HEK293T expressing AChR-GFP. Second and fifth rows: IgG, IgM, or IgA binding (red) detected through Ig-Fc specific staining. Third and sixth rows: merge with DAPI, confirming colocalization of Ig (when detected) with AChR-expressing cells. All images were captured at 63× magnification. (Scale bar: 20 μm). (*C*) Bar plots comparing detected levels of AChR-specific IgG, IgA, and IgM (ΔMFI = corrected mean fluorescence intensity) in serum sample of MG-01 and the rest of the tested cohort (n = 10). The presence of each isotype was assessed using CBAs paired with isotype Fc-specific secondary antibodies and flow cytometry. Single data point represents the mean of triplicate measurements, with error bars representing the SEM. (*D*) Schematic representation of intact AChR-IgG and AChR-IgM antibodies in serum and the corresponding cleavage products following protease treatment. Red halos denote antibodies with intact Fc domain capable of mediating effector functions, while gray symbols with crosses represent antibodies lacking Fc-mediated activity due to Fc removal. (*E*) Measurement of C3b deposition levels, after treating serum from MG-01 with S-1117 (active protease), the inactive form of S-1117, an IgM-specific protease, or a combination of S-1117 and the IgM-specific protease. C3b deposition levels are presented as normalized ΔMFI (corrected median fluorescence intensity) relative to untreated samples (ΔMFI = 1). Statistical differences are shown when significant.

The remaining samples showed variable isotype-specific contributions to complement activation, enabling classification into three distinct profiles (Fig. 5). Profile I was characterized by samples (7/21 patients, 33%) that exhibited complement deposition driven exclusively by IgG, with C3b levels mostly reduced after IgG cleavage and no significant reduction was observed after treatment of samples with the

IgM protease. Profile II was characterized by samples (6/21 patients, 28%) with complement deposition driven by both IgG and IgM, with a partial reduction in C3b levels upon treatment with either protease alone and a complete reduction after the combination treatment. Within this group, the relative contribution of each isotype varied among patients, with some exhibiting a stronger IgG contribution (patients MG-07 and MG-16), others showing a stronger IgM contribution (MG-01 and MG-10), and some displaying a comparable involvement of both isotypes (MG-09 and MG-15). Finally, profile III encompassed samples (7/21 patients, 33%) with complement deposition driven solely by IgM and C3b deposition entirely abolished following IgM degradation. Patients MG-19 and MG-20, both with longitudinal AChR-IgM-positive samples, consistently displayed this profile. Interestingly, in this category, protease treatment revealed modulatory interactions between IgG and IgM on complement activity: IgG cleavage by S-1117 either enhanced complement activation, as observed in patients MG-08 and MG-19(a and b), or partially suppressed IgM-driven complement deposition, as seen in patients MG-02 and MG-17.

To validate and extend our characterization of AChR-IgM–positive patients, we analyzed an independent cohort of 85 AChR-MG patients sampled at a single time point. Based on a positivity threshold established using healthy donor samples, 10 individuals were identified as positive for AChR-specific IgM (11.7%) (MG-C1 to MG-C10) (*SI Appendix*, Fig. S5*B*). Among these, nine samples exhibited detectable complement activation (all except MG-C10) (*SI Appendix*, Fig. S6*B*). Isotype-specific protease profiling revealed that 3 of the 9 samples (33%) matched Profile I, defined by IgG-dominant complement activity, while the remaining 6 (67%) exhibited combined IgG- and IgM-mediated activity, aligning with Profile II. Profile III, characterized by predominantly IgM-driven complement activation, was not observed in this cohort. (*SI Appendix*, Fig. S7).

To explore potential clinical correlations of AChR-IgM positivity, we integrated demographic, clinical, and laboratory data

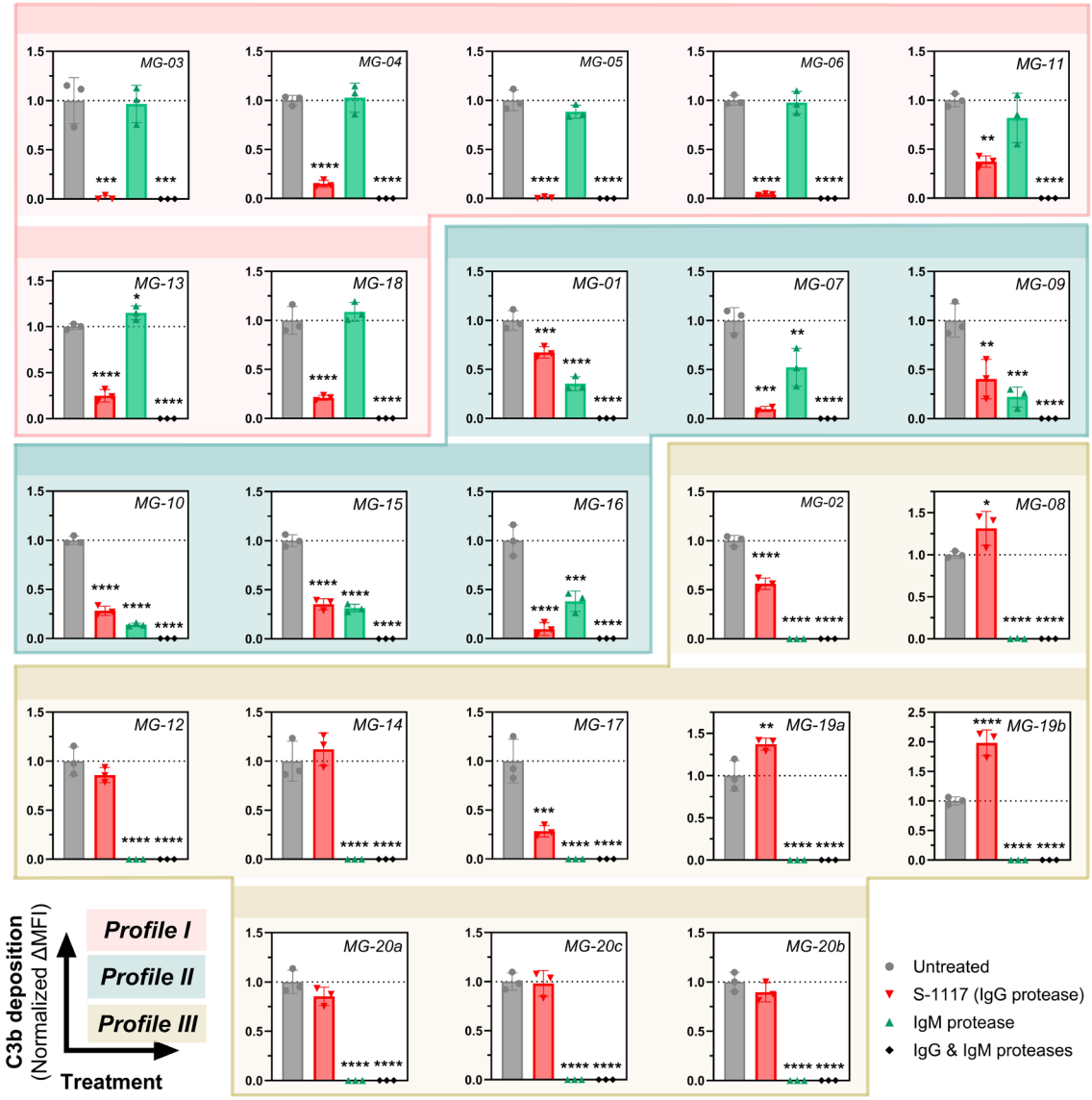

Fig. 5. AChR-IgG and IgM contribution to complement deposition in individual AChR-IgM positive serum samples. AChR-IgM positive serum samples were treated with S-1117, the IgM protease, a combination of both, or left untreated to determine AChR-IgG and IgM contribution to complement deposition. Complement deposition, measured by C3b levels, was detected using a tailored CBA and expressed as normalized ΔMFI (corrected median fluorescence intensity) relative to untreated samples (ΔMFI = 1). Individual profiles of complement-activating samples (n = 23), grouped by isotype contribution, are presented: **Profile I** (pink), complement activation mediated exclusively by IgG; **Profile II** (teal), mediated by both IgG and IgM; and **Profile III** (mustard), mediated solely by IgM. Samples from the same patient are identified by identical patient IDs with alphabetical suffixes (a, b, c) corresponding to longitudinal samples. Each condition was measured in triplicate, with error bars representing the SEM. Statistical differences versus the untreated condition are indicated when significant.

from both the primary and validation cohorts (*SI Appendix*, Table S1). Despite this comprehensive assessment, no unifying clinical or biological features were identified to distinguish this subgroup, which showed substantial heterogeneity both within and across cohorts. Collectively, these findings demonstrate that AChR-specific IgM is detectable in a subset of AChR-MG patients with heterogeneous clinical and laboratory features, and can mediate complement activation to varying extents, either in synergistic cooperation with IgG or independently, acting as a key pathogenic contributor in MG.

Discussion

Therapies targeting pathogenic autoantibodies and their effector functions have gained increased interest in autoimmune disease management. IdeS, a cysteine protease with strict IgG specificity (36–38), has shown promise by inactivating IgG-mediated mechanisms (56) central to multiple autoimmune conditions. Its potential is supported by clinical and preclinical data, including conditional European approval as Idefirix® for kidney transplant desensitization (39–42), and efficacy in models of experimental arthritis (57), immune thrombocytopenic purpura (58), Goodpasture's disease (46), neuromyelitis optica spectrum disorder (59) and Guillain–Barré syndrome (47). These studies demonstrate that IdeS efficiently cleaves IgG, thereby inhibiting complement activation and ADCC, and mitigating tissue damage and disease severity (46, 47, 57–59). However, its clinical utility is limited by rapid induction of anti-drug antibodies after a single dose, leading to enzyme neutralization, hypersensitivity, and restricted potential for repeated administration in chronic disease contexts (60).

To address this, we evaluated S-1117, a pan-IgG protease with reduced immunogenicity and extended half-life suitable for chronic use. Its activity was tested in vitro against MG-specific autoantibodies using patient-derived AChR mAbs and polyclonal serum. Five diverse, well-characterized AChR mAbs (8), along with serum from eleven previously studied subjects (20) were selected to capture varied AChR-IgG pathogenic mechanisms. Our results showed that S-1117 efficiently cleaved the Fcγ fragment from total IgG and antigen-specific autoantibodies with similar efficacy, both before and after AChR-IgG bound antigen. This dual activity suggests S-1117 can cleave circulating autoantibodies and disarm immune complexes at pathological sites, including the neuromuscular junction.

By disarming pathogenic AChR-IgG of their Fcγ domain, we expected antigen binding to remain intact, preserving Fc-independent mechanisms including AChR blocking and internalization. Our results confirmed that AChR internalization capacity was unchanged for both AChR-specific mAbs and sera. Interestingly, while blocking capacity was unaffected in the mAb assays postdigestion, a reduction was observed when testing patient sera. This discrepancy likely reflects the inherent differences between monoclonal and polyclonal systems. In the mAbs assays, the antigen is saturated by a high autoantibody load, with all mAbs sharing identical epitope specificity. Consequently, αBTX binding inhibition primarily occurs through competitive binding. In contrast, patient sera comprise a polyclonal repertoire of autoantibodies, where a fraction targets the acetylcholine binding site directly, blocking it, while others can bind proximal epitopes. These proximal autoantibodies may enhance blocking indirectly through steric hindrance caused by their Fc domains, which obstruct αBTX access.

We hypothesize that after Fcγ removal, steric hindrance contributed by the Fcγ fragment is reduced, allowing more αBTX to bind, thereby decreasing overall blocking capacity assay results. Furthermore, Fc–Fc interactions among autoantibodies recognizing distinct epitopes may stabilize autoantibody networking on antigen-rich cell surfaces, contributing to cooperative αBTX inhibition. While these mechanisms provide a plausible explanation for the observed changes, they remain hypothetical and were not pursued experimentally in the present study. It must also be emphasized that αBTX binding, while widely used, represents only an indirect approximation of antibody-mediated antagonism at the acetylcholine binding site. This assay does not always correlate with functional AChR blockade or antagonism, the large molecular size difference between acetylcholine (146 g/mol) and αBTX (~8,000 g/mol) may cause inaccurate estimates of blocking capacity. Additionally, alternative mechanisms including autoantibody-induced conformational changes, are not captured by this model (51).

While S-1117 does not directly target blocking or internalization, these mechanisms do not often represent the major or most frequent pathogenic mechanisms in AChR-MG (20). Rather, autoantibody-mediated complement deposition is observed in nearly 80% of AChR serum samples (20) and complement deposition at the neuromuscular junction (NMJ) has been reported in 85 to 100% of MG patients (4, 20, 61, 62). In this context, S-1117 exerted a consistent and pronounced effect on complement deposition. Our findings demonstrated a significant reduction in complement deposition following S-1117 treatment, observed both in assays employing AChR mAbs and serum samples, in soluble as well as antigen-bound forms. These results align with observations from in vitro studies of other autoimmune diseases, such as neuromyelitis optica (59) and Guillain–Barré syndrome (47), where antigen-specific autoantibody-mediated complement activation was effectively abolished after treatment with IdeS.

Reductions in complement deposition following S-1117-mediated cleavage were markedly greater in serum samples, ranging from 70 to 100%, compared to mAb-based assays, which averaged around 50% and peaked at 70%. Unexpectedly, increased C3b deposition was observed in assays using AChR mAbs treated with higher concentrations of S-1117 compared to those treated with minimal doses. This result led us to hypothesize that C3b deposition in the mAb system might be driven by other mechanisms, not only by AChR-bound mAbs. Complement amplification by $F(ab')_2$-immunocomplexes (ICs) has been documented (63, 64) and attributed to anti-$F(ab')_2$ antibodies including anti-hinge antibodies (AHAs) (65, 66). AHAs, identified in human sera (67, 68), selectively bind to cleaved Ig, but do not bind intact Ig (69). AHAs recognize cryptic epitopes exposed in the hinge regions of Igs following proteolytic cleavage. By binding to the hinge region, AHAs provide a surrogate Fc domain for $F(ab')_2$-ICs, capable of triggering immune effector functions, including activation of the complement cascade. To investigate whether this mechanism explained the unexpected C3b deposition increase in Fcγ-cleaved mAb samples, we preincubated NHS with S-1117 before its addition to the assay. Utilization of digested NHS abolished the increase of C3b deposition and revealed that even the lowest S-1117 dose markedly reduced complement deposition. Higher concentrations of S-1117 led to a near-complete reduction in complement deposition, as anticipated. The near-complete abrogation of complement deposition observed at 0.1 μM S-1117 can be explained by the reduction of most mAbs to scIgG under these conditions, as confirmed by our SDS-PAGE results. ScIgG has been well-documented to exhibit significantly diminished immune effector functions, including complement activation and ADCC (56, 67, 70, 71). Part of this reduction may be attributable to the lack of Fc–Fc interaction (72).

Subsequent experiments confirmed the presence of anti-F(ab′)$_2$ antibodies in NHS through their direct binding to purified, proteolytically generated F(ab′)$_2$ fragments. We refer to them collectively as anti-F(ab′)$_2$ antibodies and not AHAs, acknowledging the potential involvement of other antibodies with alternative specificities. The confirmation of the role anti-F(ab′)$_2$ antibodies played in the mAbs system raises an intriguing question: If these antibodies are consistently present in NHS and at comparable concentrations in both the mAb and serum systems for complement deposition assessment, why do they interfere with C3b deposition levels more prominently in the mAb system than in the serum samples? We reasoned that in the mAb system, all antibodies in the assay are AChR-specific, with most presenting cryptic epitopes after Fcγ cleavage. This configuration enables anti-F(ab′)$_2$ antibodies to bind to their target and form AChR-F(ab′)$_2$-ICs, promoting complement deposition and partially masking the effect of S-1117. In contrast, the polyclonal antibody repertoire in serum samples comprises a wide range of specificities, with AChR-specific autoantibodies representing only a minor fraction. Following serum sample incubation with S-1117, a large pool of non-AChR F(ab′)$_2$ fragments is generated, effectively sequestering anti-F(ab′)$_2$ antibodies away from binding to AChR-specific F(ab′)$_2$. This sequestration reduces the formation of AChR-specific F(ab′)$_2$-ICs, thereby mitigating the indirect enhancement of C3b deposition. A model illustrating this differential biological scenario in both systems is presented in *SI Appendix*, Fig. S8.

These findings, particularly those derived from our serum-based studies, indicate that S-1117 may effectively inhibit complement activation at the postsynaptic membrane of the NMJ, where pathogenic anti-AChR autoantibodies form IC with their cognate antigen. This mechanism could help mitigate skeletal muscle fiber damage, underscoring the therapeutic potential of S-1117 in preventing tissue damage associated with MG.

IgG-proteases offer a unique mechanism of action compared to traditional immunosuppressants, providing a substantial and rapid reduction of IgG antibodies within hours (60, 73, 74), ideal for acute intervention without long-term immune suppression (75, 76). In contrast to FcRn antagonists—which reduce IgG levels by blocking recycling pathways—and complement inhibitors that act downstream of immune complex formation, S-1117 exerts upstream control by directly cleaving both soluble and immune-complexed IgG, thereby preventing Fcγ receptors and C1q engagement. Notably, S-1117 also targets membrane-bound IgG, including B cell receptors, broadening its immunomodulatory profile and polypharmacological potential. Clinical trials of imlifidase—an IdeS-based therapeutic—have shown promising outcomes, with no major safety concerns or serious infections reported (40, 41). The engineered design of S-1117, incorporating immuno-silencing of T and B cell epitopes and an effector function-agnostic, autocleavage-resistant Fcγ domain, may confer additional translational advantages. Nevertheless, further rigorous preclinical studies are required to comprehensively define its pharmacodynamic and pharmacokinetic properties. Ultimately, comprehensive clinical trials will be required to evaluate therapeutic efficacy, long-term safety, and potential equivalence or superiority to existing approved treatments. Such studies will be critical to define the clinical positioning of S-1117 in future therapeutic algorithms.

Beyond its therapeutic potential, S-1117 is also a valuable research tool for dissecting the role of specific Igs in disease. In our study, Fcγ domain removal by S-1117 challenged the view that IgG is the sole driver of complement activation in MG, revealing a significant role for other isotypes—particularly IgM. Using an IgM-specific protease, we demonstrated that AChR-IgM can contribute to complement deposition in a subset of AChR-MG samples. In our primary screening cohort comprising 221 patients, 21 (9.5%) exhibited detectable levels of AChR-IgM. In an independent validation cohort, sourced from a European MG reference center, 10 out of 85 samples (11.7%) were AChR-IgM positive. These frequencies are comparable with each other and fall within previously reported ranges (19, 20). Within the AChR-IgM positive subset, one patient in each cohort showed no detectable complement activity. Notably, these samples also showed the lowest levels of AChR-IgG binding, consistent with previous findings indicating a positive correlation between autoantibody binding and complement activity (20, 77).

Among the complement-activating samples harboring AChR-specific IgG and IgM autoantibodies, three distinct profiles of isotype-mediated complement activity were identified. In Profile I, complement activity was exclusively mediated by IgG, as evidenced by a significant reduction of complement following IgG cleavage but no implication of IgM. Profile II exhibited complement activity mediated by both IgG and IgM, with significant but partial reductions in complement levels observed upon treatment with either protease alone and complete abrogation following combined protease treatment. Finally, Profile III demonstrated complement activity predominantly driven by IgM, with complement activation fully suppressed after IgM cleavage alone. While all three profiles were represented in the primary cohort, only Profiles I and II were identified in the validation cohort. Differences in profile frequencies between cohorts were also noted. These variations are not unexpected and may reflect several factors. First, the smaller sample size in the validation cohort reduces the likelihood of detecting profiles identified in larger screening cohorts. Second, variations in cohort composition—including disease stage, MG subclass (EOMG, LOMG, TAMG) and treatment status—can influence the presence, abundance, and effector potential of autoantibody isotypes. Third, given the inherent biological heterogeneity of MG and the complex interplay between autoantibody classes and complement activation, degrees of intercohort variability are anticipated.

Isotype-specific protease treatments also provided valuable insights into the intricate interactions between IgG and IgM and their respective contributions to complement activity. In some Profile II samples, the cleavage of either IgG or IgM alone significantly reduced complement activity, though the reductions were not necessarily proportional or additive, indicating functional interdependence. In Profile III, IgG cleavage led to either significant enhanced or diminished complement activity compared to the untreated condition. These effects may stem from reduced steric hindrance, increasing accessibility for the competing isotype and subsequent augmented complement activity, or from disrupted cooperative interactions between isotypes affecting immunocomplex orientation and stability and thus, reduced complement activity. Additionally, the loss of synergistic support between isotypes could lead to suboptimal binding configurations. These findings underscore the distinct yet interdependent roles of IgG and IgM in complement activation, establish the pathogenic significance of AChR-IgM in MG, and identify a subset of patients unlikely to benefit from IgG-centered therapies, such as FcRn inhibitors, necessitating tailored treatment strategies. These results align with emerging evidence implicating IgM in traditionally IgG-driven autoimmune diseases, such as bullous pemphigoid (78) and rheumatoid arthritis (79), suggesting the broader

applicability of isotype-specific proteases in treating other autoimmune conditions. Finally, the data support adapting clinical AChR autoantibody testing assays to measure both IgG and IgM, enabling the identification of such patients and the application of appropriate therapeutic strategies.

Our study is not without limitations. First, while distinct complement activation profiles were identified, caution is warranted when extrapolating their exact prevalence to the broader MG population, and additional unrecognized immunopathologic profiles may also exist. In addition, despite being one of the largest MG cohorts analyzed for AChR-IgM, the number of IgM-positive cases is underpowered for definitive clinical correlations. Furthermore, while our investigation elucidates IgM role in complement activation, its broader role in MG pathology remains undefined, warranting further investigation into IgM-specific mechanisms relative to IgG. Last, our investigation did not assess the capacity of the IgG protease to cleave B cell receptors, which may have significant implications for disease dynamics reinforcing the therapeutic potential of S-1117 in the context of MG.

We identify IgM as a pivotal molecular contributor in the immunopathology of MG. Our findings uncover a patient subset characterized by IgM-driven complement activation, for whom conventional IgG-centered therapeutic approaches, such as FcRn inhibition, may prove insufficient. Furthermore, these results underscore the broader pathogenic complexity of MG heterogeneity. In this context, evaluating antigen-specific Ig profiles beyond the traditional IgG focus is imperative. However, the detection of a given isotype does not inherently indicate pathogenic relevance; functional characterization through effector potential is essential to determine disease involvement. The contribution of multiple Ig classes suggests the potential for diverse clinical profiles in MG, reinforcing the need for personalized therapeutic strategies. Although agents like S-1117 selectively inhibit Fcγ-mediated pathways, the challenge of aligning patients with appropriate immunomodulatory therapies applies broadly—including complement inhibitors and FcRn blockers—whose efficacy depends on underlying immune mechanisms. Clinical integration of functional assays capable of dissecting these mechanisms will be critical for precise patient stratification, rational treatment selection, optimization of healthcare resource utilization, and avoidance of unnecessary therapeutic exposure. Moreover, this mechanistic profiling supports the rationale for combination therapies to effectively address MG complexity among diverse patient populations.

Materials and Methods

To assess the therapeutic efficacy of the IgG-specific protease S–1117, 5 recombinant AChR-IgG mAbs (8) and sera from 11 AChR-MG patients (20) were treated with S–1117 or an inactive protease and evaluated via ELISA and live CBA for Fcγ removal. Pathogenic effector functions were assessed using customized CBAs. Samples with residual complement activity post-IgG cleavage uncovered AChR-IgM involvement confirmed using an IgM-specific protease. Additional screening of 330 AChR-MG samples (210 patients), 78 MuSK-MG, and 48 healthy donors, plus validation in an independent cohort of 85 patients, identified 31 AChR-IgM+ cases. Functional stratification via protease treatments and CBA profiling defined isotype-specific contributions to complement activation. Detailed description available in *SI Appendix*.

Data, Materials, and Software Availability. All study data are included in the article and/or *SI Appendix*.

ACKNOWLEDGMENTS. We thank Drs. Vanda A. Lennon and John R. Mills (Mayo Clinic) for mcAb-3; Drs. Angela Vincent, David Beeson, and Patrick Waters (University of Oxford) for AChR subunit plasmids; and Dr. Jeffrey L. Bennett (University of Colorado) for the AQP4-specific mAb58. We also thank Julia Manasson and John Sundy for their feedback, Ishan Sharma for antibody production and purification, and all members of the Seismic team for their contributions to creating a scientifically rigorous and patient-motivated workplace.

Author affiliations: [a]Department of Neurology, Yale School of Medicine, New Haven, CT 06511; [b]Department of Immunobiology, Yale School of Medicine, New Haven, CT 06511; [c]Seismic Therapeutic, Watertown, MA 02472; and [d]Department of Neurosciences, Drugs and Child Health, University of Florence, Florence 50139, Italy

Author contributions: A.C.B., L.M.S., A. Pellerin, H.V., K.L.O., I.D.M., and K.C.O. designed research; A.C.B., L.M.S., A. Pellerin, G.M., A. Plasencia, J.M.A., K.L.O., and Y.X. performed research; R.J.N., V.D., L.M., M.C.P., F.K.-H., and N.H.-S. contributed new reagents/analytic tools; A.C.B., L.M.S., K.L.O., and Y.X. analyzed data; A.C.B., L.M.S., A. Pellerin, G.M., A. Plasencia, R.J.N., V.D., L.M., M.C.P., F.K.-H., N.H.-S., and Y.X. reviewed & edited the manuscript; H.V. supervised project and reviewed & edited manuscript; I.D.M. supervised and administered the project, reviewed & edited the manuscript; K.C.O. acquired funding, supervised and administered the project, reviewed & edited the manuscript; and A.C.B. and K.C.O. wrote the paper.

Competing interest statement: K.C.O. is an equity shareholder of Cabaletta Bio; serves on advisory boards for Roche, Merck (EMD Serono), Neurocrine Biosciences and Seismic Therapeutic; and has received research support from Viela Bio, (now Horizon Therapeutics/Amgen), argenx, and Seismic Therapeutic. R.J.N. has received research support from the NIH, Genentech, Inc., Alexion Pharmaceuticals, Inc., argenx, Annexon Biosciences, Inc., Ra Pharmaceuticals, Inc. (now UCB S.A.), the Myasthenia Gravis Foundation of America, Inc., Momenta Pharmaceuticals, Inc. (now Janssen), Immunovant, Inc., Grifols, S.A., and Viela Bio, Inc. (Horizon Therapeutics, now Amgen Inc.). R.J.N. has served as a consultant and advisor for Alexion Pharmaceuticals, Inc., argenx, Cabaletta Bio, Inc., Cour Pharmaceuticals, Ra Pharmaceuticals, Inc. (now UCB S.A.), Immunovant, Inc., Momenta Pharmaceuticals, Inc. (now Janssen), and Viela Bio, Inc. (Horizon Therapeutics, now Amgen Inc.). The rest of authors have declared that no conflict of interest exists. This study was supported by the National Institute of Allergy and Infectious Diseases (NIAID) of the NIH under award numbers R01-AI114780 and R21-AI164590 (to K.C.O.). A.C.B. was supported, in part, through an MGNet Scholar award provided by the Rare Diseases Clinical Research Consortia of the NIH and MGNet, under award number U54-NS115054. Additional support was provided by Seismic Therapeutic to K.C.O.

1. J. M. Lindstrom, M. E. Seybold, V. A. Lennon, S. Whittingham, D. D. Duane, Antibody to acetylcholine receptor in myasthenia gravis. Prevalence, clinical correlates, and diagnostic value. *Neurology* **26**, 1054–1059 (1976).
2. L. Jacobson, D. Beeson, S. Tzartos, A. Vincent, Monoclonal antibodies raised against human acetylcholine receptor bind to all five subunits of the fetal isoform. *J. Neuroimmunol.* **98**, 112–120 (1999).
3. F. M. Howard Jr., V. A. Lennon, J. Finley, J. Matsumoto, L. R. Elveback, Clinical correlations of antibodies that bind, block, or modulate human acetylcholine receptors in myasthenia gravis. *Ann. N. Y. Acad. Sci.* **505**, 526–538 (1987).
4. M. Tsujihata *et al.*, Diagnostic significance of IgG, C3, and C9 at the limb muscle motor end-plate in minimal myasthenia gravis. *Neurology* **39**, 1359–1363 (1989).
5. A. G. Engel *et al.*, Passively transferred experimental autoimmune myasthenia gravis. Sequential and quantitative study of the motor end-plate fine structure and ultrastructural localization of immune complexes (IgG and C3), and of the acetylcholine receptor. *Neurology* **29**, 179–188 (1979).
6. S. Heinemann, S. Bevan, R. Kullberg, J. Lindstrom, J. Rice, Modulation of acetylcholine receptor by antibody against the receptor. *Proc. Natl. Acad. Sci. U.S.A.* **74**, 3090–3094 (1977).
7. R. R. Almon, C. G. Andrew, S. H. Appel, Serum globulin in myasthenia gravis: Inhibition of alpha-bungarotoxin binding to acetylcholine receptors. *Science* **186**, 55–57 (1974).
8. M. C. Pham *et al.*, Individual myasthenia gravis autoantibody clones can efficiently mediate multiple mechanisms of pathology. *Acta Neuropathol.* **146**, 319–336 (2023).
9. N. Rose *et al.*, Receptor clustering and pathogenic complement activation in myasthenia gravis depend on synergy between antibodies with multiple subunit specificities. *Acta Neuropathol.* **144**, 1005–1025 (2022).
10. K. Vrolix *et al.*, Clonal heterogeneity of thymic B cells from early-onset myasthenia gravis patients with antibodies against the acetylcholine receptor. *J. Autoimmun.* **52**, 101–112 (2014).
11. K. Lazaridis, S. J. Tzartos, Autoantibody specificities in myasthenia gravis; Implications for improved diagnostics and therapeutics. *Front. Immunol.* **11**, 212 (2020).
12. A. Vincent, J. Newsom-Davis, Acetylcholine receptor antibody characteristics in myasthenia gravis. I. Patients with generalized myasthenia or disease restricted to ocular muscles. *Clin. Exp. Immunol.* **49**, 257–265 (1982).
13. A. K. Lefvert, S. Cuenoud, B. W. Fulpius, Binding properties and subclass distribution of anti-acetylcholine receptor antibodies in myasthenia gravis. *J. Neuroimmunol.* **1**, 125–135 (1981).
14. K. V. Toyka *et al.*, Study of humoral immune mechanisms by passive transfer to mice. *N. Engl. J. Med.* **296**, 125–131 (1977).
15. A. Rodgaard, F. C. Nielsen, R. Djurup, F. Somnier, S. Gammeltoft, Acetylcholine receptor antibody in myasthenia gravis: Predominance of IgG subclasses 1 and 3. *Clin. Exp. Immunol.* **67**, 82–88 (1987).
16. A. Vincent, J. Newsom Davis, Anti-acetylcholine receptor antibodies. *J. Neurol. Neurosurg. Psychiatry* **43**, 590–600 (1980).
17. A. K. Lefvert, Immunoglobulins in myasthenia gravis. Kinetic properties of the acetylcholine-receptor antibody studied during lymph drainage. *Clin. Exp. Immunol.* **34**, 111–117 (1978).
18. H. Link *et al.*, Acetylcholine receptor-reactive T and B cells in myasthenia gravis and controls. *J. Clin. Invest.* **87**, 2191–2196 (1991).
19. R. S. Tindall, Humoral immunity in myasthenia gravis: Biochemical characterization of acquired antireceptor antibodies and clinical correlations. *Ann. Neurol.* **10**, 437–447 (1981).
20. F. Khani-Habibabadi *et al.*, AChR autoantibody pathogenic properties are heterogeneously distributed and undergo temporal changes among patients with myasthenia gravis. *Neurol. Neuroimmunol. Neuroinflamm.* **12**, e200436 (2025).

21. J. F. Howard Jr. *et al.*, Safety and efficacy of zilucoplan in patients with generalised myasthenia gravis (RAISE): A randomised, double-blind, placebo-controlled, phase 3 study. *Lancet Neurol.* **22**, 395–406 (2023).
22. A. Meisel *et al.*, Long-term efficacy and safety of ravulizumab in adults with anti-acetylcholine receptor antibody-positive generalized myasthenia gravis: Results from the phase 3 CHAMPION MG open-label extension. *J. Neurol.* **270**, 3862–3875 (2023).
23. J. F. Howard Jr. *et al.*, Safety and efficacy of eculizumab in anti-acetylcholine receptor antibody-positive refractory generalised myasthenia gravis (REGAIN): A phase 3, randomised, double-blind, placebo-controlled, multicentre study. *Lancet Neurol.* **16**, 976–986 (2017).
24. J. F. Howard Jr. *et al.*, Safety, efficacy, and tolerability of efgartigimod in patients with generalised myasthenia gravis (ADAPT): A multicentre, randomised, placebo-controlled, phase 3 trial. *Lancet Neurol.* **20**, 526–536 (2021).
25. V. Bril *et al.*, Safety and efficacy of rozanolixizumab in patients with generalised myasthenia gravis (MycarinG): A randomised, double-blind, placebo-controlled, adaptive phase 3 study. *Lancet Neurol.* **22**, 383–394 (2023).
26. J. Vissing *et al.*, "Minimal symptom expression" in patients with acetylcholine receptor antibody-positive refractory generalized myasthenia gravis treated with eculizumab. *J. Neurol.* **267**, 1991–2001 (2020).
27. T. Vu *et al.*, Terminal complement inhibitor ravulizumab in generalized myasthenia gravis. *N. Engl. J. Med. Evid.* **1**, EVIDoa2100066 (2022).
28. F. Stascheit *et al.*, Ravulizumab and efgartigimod in myasthenia gravis: A real-world study. *Neurol. Neuroimmunol. Neuroinflamm.* **12**, e200331 (2025).
29. D. Barth, M. Nabavi Nouri, E. Ng, P. Nwe, V. Bril, Comparison of IVIg and PLEX in patients with myasthenia gravis. *Neurology* **76**, 2017–2023 (2011).
30. E. M. Bershad, E. S. Feen, J. I. Suarez, Myasthenia gravis crisis. *South. Med. J.* **101**, 63–69 (2008).
31. D. B. Sanders *et al.*, International consensus guidance for management of myasthenia gravis: Executive summary. *Neurology* **87**, 419–425 (2016).
32. A. Mullard, Extracellular targeted protein degrader removes antibodies in first test in humans. *Nat. Rev. Drug Discov.* **23**, 483–486 (2024).
33. J. A. Wells, K. Kumru, Extracellular targeted protein degradation: An emerging modality for drug discovery. *Nat. Rev. Drug Discov.* **23**, 126–140 (2024).
34. U. von Pawel-Rammingen, B. P. Johansson, H. Tapper, L. Bjorck, *Streptococcus pyogenes* and phagocytic killing. *Nat. Med.* **8**, 1044–1045 (2002).
35. B. Vincents, U. von Pawel-Rammingen, L. Bjorck, M. Abrahamson, Enzymatic characterization of the streptococcal endopeptidase, IdeS, reveals that it is a cysteine protease with strict specificity for IgG cleavage due to exosite binding. *Biochemistry* **43**, 15540–15549 (2004).
36. P. Akesson, L. Moritz, M. Truedsson, B. Christensson, U. von Pawel-Rammingen, Ides, a highly specific immunoglobulin G (IgG)-cleaving enzyme from Streptococcus pyogenes, is inhibited by specific IgG antibodies generated during infection. *Infect. Immun.* **74**, 497–503 (2006).
37. U. von Pawel-Rammingen, B. P. Johansson, L. Bjorck, IdeS, a novel streptococcal cysteine proteinase with unique specificity for immunoglobulin G. *EMBO J.* **21**, 1607–1615 (2002).
38. K. Wenig *et al.*, Structure of the streptococcal endopeptidase IdeS, a cysteine proteinase with strict specificity for IgG. *Proc. Natl. Acad. Sci. U.S.A.* **101**, 17371–17376 (2004).
39. B. E. Lonze *et al.*, IdeS (imlifidase): A novel agent that cleaves human IgG and permits successful kidney transplantation across high-strength donor-specific antibody. *Ann. Surg.* **268**, 488–496 (2018).
40. S. C. Jordan *et al.*, Imlifidase desensitization in crossmatch-positive, highly sensitized kidney transplant recipients: Results of an international phase 2 trial (Highdes). *Transplantation* **105**, 1808–1817 (2021).
41. S. C. Jordan *et al.*, IgG endopeptidase in highly sensitized patients undergoing transplantation. *N. Engl. J. Med.* **377**, 442–453 (2017).
42. C. Kjellman *et al.*, Outcomes at 3 years posttransplant in imlifidase-desensitized kidney transplant patients. *Am. J. Transplant.* **21**, 3907–3918 (2021).
43. M. Kanbay *et al.*, Imlifidase in kidney transplantation. *Clin. Kidney J.* **17**, sfae033 (2024).
44. M. Segelmark, F. Uhlin, E. Sonesson, The immunoglobulin G degrading enzyme imlifidase for the treatment of anti-GBM disease: The GOOD-IDES 01 trial. *J. Am. Soc. Nephrol.* **31**, B9–B9 (2020).
45. F. Uhlin *et al.*, Endopeptidase cleavage of anti-glomerular basement membrane antibodies in vivo in severe kidney disease: An open-label phase 2a study. *J. Am. Soc. Nephrol.* **33**, 829–838 (2022).
46. R. Yang *et al.*, Successful treatment of experimental glomerulonephritis with IdeS and EndoS, IgG-degrading streptococcal enzymes. *Nephrol. Dial. Transplant.* **25**, 2479–2486 (2010).
47. R. Takahashi, N. Yuki, Streptococcal ides: Therapeutic potential for Guillain–Barre syndrome. *Sci. Rep.* **5**, 10809 (2015).
48. U. von Pawel-Rammingen, Streptococcal IdeS and its impact on immune response and inflammation. *J. Innate Immun.* **4**, 132–140 (2012).
49. A. Norrby-Teglund *et al.*, Evidence for the presence of streptococcal-superantigen-neutralizing antibodies in normal polyspecific immunoglobulin G. *Infect. Immun.* **64**, 5395–5398 (1996).
50. P. F. Kennel, P. Poindron, J. M. Warter, P. Fonteneau, Alpha-Bungarotoxin sensitization in experimental autoimmune myasthenia gravis. *Muscle Nerve* **16**, 461–465 (1993).
51. H. Li *et al.*, Autoimmune mechanisms elucidated through muscle acetylcholine receptor structures. *Cell* **188**, 2390–2406.e20 (2025).
52. V. A. Lennon, E. H. Lambert, Myasthenia gravis induced by monoclonal antibodies to acetylcholine receptors. *Nature* **285**, 238–240 (1980).
53. M. Basta, Ambivalent effect of immunoglobulins on the complement system: Activation versus inhibition. *Mol. Immunol.* **45**, 4073–4079 (2008).
54. M. C. Dalakas, H. Alexopoulos, P. J. Spaeth, Complement in neurological disorders and emerging complement-targeted therapeutics. *Nat. Rev. Neurol.* **16**, 601–617 (2020).
55. T. H. Sharp *et al.*, Insights into IgM-mediated complement activation based on in situ structures of IgM-C1-C4b. *Proc. Natl. Acad. Sci. U.S.A.* **116**, 11900–11905 (2019).
56. R. J. Brezski *et al.*, Tumor-associated and microbial proteases compromise host IgG effector functions by a single cleavage proximal to the hinge. *Proc. Natl. Acad. Sci. U.S.A.* **106**, 17864–17869 (2009).
57. K. S. Nandakumar, B. P. Johansson, L. Bjorck, R. Holmdahl, Blocking of experimental arthritis by cleavage of IgG antibodies in vivo. *Arthritis Rheum.* **56**, 3253–3260 (2007).
58. B. P. Johansson, O. Shannon, L. Bjorck, IdeS: A bacterial proteolytic enzyme with therapeutic potential. *PLoS One* **3**, e1692 (2008).
59. L. Tradtrantip, N. Asavapanumas, A. S. Verkman, Therapeutic cleavage of anti-aquaporin-4 autoantibody in neuromyelitis optica by an IgG-selective proteinase. *Mol. Pharmacol.* **83**, 1268–1275 (2013).
60. L. Winstedt *et al.*, Complete removal of extracellular IgG antibodies in a randomized dose-escalation phase I study with the bacterial enzyme IdeS–a novel therapeutic opportunity. *PLoS One* **10**, e0132011 (2015).
61. S. Nakano, A. G. Engel, Myasthenia gravis: Quantitative immunocytochemical analysis of inflammatory cells and detection of complement membrane attack complex at the end-plate in 30 patients. *Neurology* **43**, 1167–1172 (1993).
62. A. G. Engel, E. H. Lambert, F. M. Howard, Immune complexes (IgG and C3) at the motor end-plate in myasthenia gravis: Ultrastructural and light microscopic localization and electrophysiologic correlations. *Mayo Clin. Proc.* **52**, 267–280 (1977).
63. T. Fujita, M. Takiuchi, K. Iida, K. Nagaki, S. Inai, The activation mechanism of the alternative pathway of the human complement system by the immune precipitate formed with F(ab')2 of rabbit IgG antibody: The generation of C3- and C5-cleaving enzymes on the immune precipitate. *Immunochemistry* **14**, 25–30 (1977).
64. K. B. Reid, Complement fixation by the F(ab')2-fragment of pepsin-treated rabbit antibody. *Immunology* **20**, 649–658 (1971).
65. R. J. Brezski, R. E. Jordan, Cleavage of IgGs by proteases associated with invasive diseases: An evasion tactic against host immunity? *MAbs* **2**, 212–220 (2010).
66. R. J. Brezski *et al.*, A monoclonal antibody against hinge-cleaved IgG restores effector function to proteolytically-inactivated IgGs in vitro and in vivo. *MAbs* **6**, 1265–1273 (2014).
67. R. J. Brezski *et al.*, Human anti-IgG1 hinge autoantibodies reconstitute the effector functions of proteolytically inactivated IgGs. *J. Immunol.* **181**, 3183–3192 (2008).
68. C. K. Osterland, M. Harboe, H. G. Kunkel, Anti-gamma-globulin factors in human sera revealed by enzymatic splitting of anti-Rh antibodies. *Vox Sang.* **8**, 133–152 (1963).
69. T. Huang *et al.*, Molecular characterization of human anti–hinge antibodies derived from single-cell cloning of normal human B cells. *J. Biol. Chem.* **293**, 906–919 (2018).
70. R. J. Brezski, D. M. Knight, R. E. Jordan, The origins, specificity, and potential biological relevance of human anti–IgG hinge autoantibodies. *ScientificWorldJournal* **11**, 1153–1167 (2011).
71. X. Fan *et al.*, A single proteolytic cleavage within the lower hinge of trastuzumab reduces immune effector function and in vivo efficacy. *Breast Cancer Res.* **14**, R116 (2012).
72. J. Soltys *et al.*, Membrane assembly of aquaporin-4 autoantibodies regulates classical complement activation in neuromyelitis optica. *J. Clin. Invest.* **129**, 2000–2013 (2019).
73. T. Lorant *et al.*, Safety, immunogenicity, pharmacokinetics, and efficacy of degradation of anti-HLA antibodies by IdeS (imlifidase) in chronic kidney disease patients. *Am. J. Transplant.* **18**, 2752–2762 (2018).
74. I. Soveri *et al.*, The IgG-degrading enzyme of *Streptococcus pyogenes* causes rapid clearance of anti-glomerular basement membrane antibodies in patients with refractory anti-glomerular basement membrane disease. *Kidney Int.* **96**, 1234–1238 (2019).
75. D. R. Lynch *et al.*, Anchoring IgG-degrading enzymes to the surface of platelets selectively neutralizes antiplatelet antibodies. *Blood Adv.* **6**, 4645–4656 (2022).
76. C. Rafat, Y. Luque, Ides in anti-glomerular basement membrane disease: Is this the new deal? *Kidney Int.* **96**, 1068–1070 (2019).
77. A. H. Obaid *et al.*, Heterogeneity of acetylcholine receptor autoantibody-mediated complement activity in patients with myasthenia gravis. *Neurol. Neuroimmunol. Neuroinflamm.* **9**, e1169 (2022).
78. Y. Hirano *et al.*, Super-resolution imaging detects BP180 autoantigen in immunoglobulin M pemphigoid. *J. Dermatol.* **49**, 374–378 (2022).
79. S. Reijm *et al.*, Cross-reactivity of IgM anti-modified protein antibodies in rheumatoid arthritis despite limited mutational load. *Arthritis Res. Ther.* **23**, 230 (2021).